

Keywords: PDE4D7; PDE4D; prostate cancer; cAMP; cyclic adenosine mono-phosphate

The cAMP phosphodiesterase-4D7 (PDE4D7) is downregulated in androgen-independent prostate cancer cells and mediates proliferation by compartmentalising cAMP at the plasma membrane of VCaP prostate cancer cells

D J P Henderson^{1,5}, A Byrne^{1,5}, K Dulla², G Jenster³, R Hoffmann², G S Baillie^{*1} and M D Houslay⁴

¹Institute of Cardiovascular and Medical Sciences, University of Glasgow, 126 University Place, Glasgow G12 8TA, UK;

²Philips Research Eindhoven, Molecular Diagnostics, HTC11.1.165, 5656AE Eindhoven, The Netherlands; ³Erasmus MC, PO box 2040, 3000 CA Rotterdam, The Netherlands and ⁴Institute of Pharmaceutical Science, KCL, Franklin-Wilkins Building, 150 Stamford Street, London SE1 9NH, UK

Background: Isoforms of the PDE4 family of cAMP-specific phosphodiesterases (PDEs) are expressed in a cell type-dependent manner and contribute to underpinning the paradigm of intracellular cAMP signal compartmentalisation. Here we identify the differential regulation of the PDE4D7 isoform during prostate cancer progression and uncover a role in controlling prostate cancer cell proliferation.

Methods: PDE4 transcripts from 19 prostate cancer cell lines and xenografts were quantified by qPCR. PDE4D7 expression was further investigated because of its significant downregulation between androgen-sensitive (AS) and androgen-insensitive (AI) samples. Western blot analysis, PDE activity assay, immunofluorescent staining and cAMP responsive FRET assays were used to investigate the sub-plasma membrane localisation of a population of PDE4D7 in VCaP (AS) and PC3 (AI) cell lines. Disruption of this localisation pattern using dominant-negative protein expression and siRNA knockdown showed that PDE4D7 acts in opposition to proliferative signalling as assessed by electrical impedance-based proliferation assays.

Results: Here we identify the differential regulation of the PDE4D7 isoform during prostate cancer progression. PDE4D7 is highly expressed in AS cells and starkly downregulated in AI samples. The significance of this downregulation is underscored by our finding that PDE4D7 contributes a major fraction of cAMP degrading PDE activity tethered at the plasma membrane and that displacement of PDE4D7 from this compartment leads to an increase in the proliferation of prostate cancer cells. PDE4D7 mRNA expression is not, however, directly regulated by the androgen receptor signalling axis despite an overlapping genomic structure with the androgen responsive gene *PART1*. PDE4D7, which localises to the plasma membrane, acts to suppress aberrant non-steroidal growth signals within the prostate or AS metastasis.

Conclusions: PDE4D7 expression is significantly downregulated between AS and AI cell phenotypes. This change in expression potentially provides a novel androgen-independent biomarker and manipulation of its activity or its expression may provide therapeutic possibilities and insights into contributory aspects of the complex molecular pathology of prostate cancer.

*Correspondence: Professor GS Baillie; E-mail: George.Baillie@Glasgow.ac.uk

⁵These authors contributed equally to this work.

Received 6 September 2013; revised 20 December 2013; accepted 7 January 2014; published online 11 February 2014

© 2014 Cancer Research UK. All rights reserved 0007–0920/14

Prostate cancer is the second most commonly diagnosed malignancy in men (Siegel *et al*, 2013). The majority of prostate cancer cases arise within the epithelial lumen of the prostate and are dependent upon androgens for proliferation (Grignon and Sakr, 1994; Wang *et al*, 2009). The treatment of prostatic tumours initially revolves around the deprivation of androgens. This palliative treatment regime leads to a well-characterised remission in the mass and exhibited symptoms of prostatic adenocarcinoma (Foley *et al*, 2011). However, this initial remission is invariably followed by the emergence and expansion of tumour cells that no longer depend upon the canonical androgen signalling axis to drive proliferation and disease progression (Feldman and Feldman, 2001). There is great interest in trying to determine the nature of the molecular events surrounding the progression into androgen-insensitive (AI) cell phenotype (Wegiel *et al*, 2010).

It has been reported that differential G_s-coupled GPCR signalling, PKA catalytic subunit switching and adenylyl cyclase isoform expression are observed between the androgen-sensitive (AS) and AI cancer phenotypes (Kasbohm *et al*, 2005; Kvissel *et al*, 2007; Flacke *et al*, 2013), implying that alterations in the regulation of cAMP signalling cascades are an important factor in prostate cancer progression (Merkle and Hoffmann, 2011). The actions of the ubiquitous second messenger cAMP are governed by the processes of spatially distinct synthesis and degradation where adenylyl cyclases mediate the synthesis of cAMP, and cyclic nucleotide phosphodiesterases (PDEs) represent the only known means by which cAMP is degraded in cells (Houslay, 2010).

There are 11 families of cyclic nucleotide PDEs, of which 3 are able to specifically hydrolyse cAMP, 5 hydrolyse both cAMP and cGMP and the remaining families are specific for cGMP (Francis *et al*, 2011). Complex mechanisms of isoform expression within these families are coupled with different modes of enzymatic regulation to underpin the paradigm of compartmentalised cAMP signalling (Houslay, 2010; Francis *et al*, 2011). The PDE4 family of cAMP-specific PDEs are of particular note for their described regulatory functions and expression patterns (Houslay and Adams, 2003; Conti and Beavo, 2007). From four genes (PDE4A/B/C/D), a series of isoforms are encoded with distinct N-terminal regions shown to be invariably associated with targeting to specific intracellular sites and signalling complexes (Huston *et al*, 2006; Lynch *et al*, 2007; Keravis and Lugnier, 2010; MacKenzie *et al*, 2011; Murdoch *et al*, 2011). This form of compartmentalisation allows multiple signalling events to be independently regulated in temporally and spatially distinct intracellular locales. Therefore, dysregulation of PDE-mediated cAMP compartmentalisation may underpin abrogation of cellular function in disease states (Houslay *et al*, 2007; Houslay, 2010).

In this study, we set out to determine if the expression levels of PDE4 isoform variants are altered during the AS to AI transition and if this has consequences for cellular proliferation. The mRNA expression levels of PDE4 families and isoform variants were evaluated in 19 prostate cancer cell lines and xenografts and our analysis uncovered that total PDE4D mRNA levels are decreased during the AS to AI transition. Further investigation revealed that a significant proportion of this decrease is due to decreasing PDE4D7 expression, and that this is sustained at protein level leading to a reduced ability for prostate cancer cells to hydrolyse cAMP. We also describe how a population of PDE4D7 exhibits a targeted localisation pattern and regulates a sub-plasma membrane cAMP compartment. Crucially, we find that disruption of this compartmentalisation leads to an increase in cellular proliferation. Last, we describe how the expression of PDE4D7 is regulated outside the control of canonical androgen signalling, despite the unique exon composition of PDE4D7 overlapping with a previously described androgen responsive gene, namely prostate androgen-regulated transcript-1 (*PART1*; Lin *et al*, 2000).

MATERIALS AND METHODS

Materials. Forskolin, 3-isobutyl-1-methylxanthine (IBMX), rolipram, dihydrotestosterone and hydroxyflutamide were purchased from Sigma (Gillingham, UK). PDE4D-specific antisera were described previously (MacKenzie *et al*, 2002), anti-GFP and GP130 antisera were purchased from Abcam (Cambridge, UK) and anti vsv-tag antisera from Sigma. A PDE4D7 antibody was raised against a peptide mapping the unique N-terminal region of PDE4D7 and specificity was assessed against peptide array.

Molecular biology. PDE4D7 was sub-cloned into pGFP-N1 (Clontech, Mountain View, CA, USA) and pcDNA3.1 (Life Technologies, Paisley, UK) and tagged with a VSV epitope label. A dominant negative D559A mutation was introduced to the PDE4D7 expression construct using Quickchange site-directed mutagenesis kit (Stratagene, La Jolla, CA, USA; McCahill *et al*, 2005). Targeted cAMP responsive FRET probes were a kind gift from Professor M Zaccolo (Oxford, UK; Terrin *et al*, 2006). Pluc luciferase constructs were purchased from Origene (Rockville, MD, USA) and Renilla pRL-TK from Promega (Madison, WI, USA). Promoter regions cloned from genomic DNA prepared from VCaP cells using a high salt extraction buffer (10 mM Tris, pH 7.5, 400 mM NaCl, 100 mM EDTA, 0.6% SDS), protein precipitated with 6 M NaCl before precipitation of DNA using one sample volume of 100% ethanol. Amplification of genomic regions was carried out with platinum pfx polymerase from Life Technologies. Sequence data for all oligonucleotides used in this study can be found in Supplementary Table 1.

Mammalian cell culture. VCaP, LNCaP, PC3 and DU145 prostate cancer cell lines were purchased from ATCC (Teddington, UK) and were maintained in RPMI1640 supplemented with 10% FBS, whereas DU145 cells were cultured in DMEM supplemented with 10% FBS. Transfections were carried out using Lipofectamine 2000 (Life Technologies) as per the manufacturer's instruction. Serum and media were purchased from Sigma. siRNA against PDE4D7 (5'-AUACCUGUGAUUUGCUUUC-3', targeting the unique N-terminal region of PDE4D7) and panPDE4D (Lynch *et al*, 2005) were purchased from Ambion (Life Technologies).

RT-qPCR. Total RNA from human prostate cancer cell lines and xenografts were a kind gift from Guido Jenster of Erasmus Medical Centre, Rotterdam, The Netherlands. Additional total RNA was harvested using Trizol (Life Technologies) according to the manufacturer's instruction, DNase treated (Roche, Welwyn Garden City, UK) followed by on column purification using RNeasy RNA extraction kit (Qiagen, Manchester, UK). First-strand cDNA synthesis was carried out on 500 ng total RNA using superscript VILO and random hexamer oligonucleotide primers (Life Technologies). qPCR reactions were conducted using the ABI Prism 7300 qPCR thermocycler and analysis software (60 °C 30 s, 95 °C 10 min followed by 40 cycles of 95 °C 15 s, 60 °C 1 min). Reactions were conducted in qPCR Fastmix (VWR, Lutterworth, UK). The primers used in this study can be found in Supplementary Information and were sourced from Eurofins MWG Operon (Ebersberg, Germany). Final primer concentration used in RT-qPCR was 250 nM. Data analysis was conducted using GAPDH expression as an internal reference after ensuring its stable expression throughout the sample set.

Protein biochemistry and western blotting. Immunoprecipitations and western blots for PDE4D7 were carried out as previously described (MacKenzie *et al*, 2011), using antisera raised against the N-terminal regions of PDE4D7 (Baillie Laboratory, Glasgow, UK), western blotting was conducted using previously described antisera against PDE4D (MacKenzie *et al*, 2002). Western blots were analysed using HRP-conjugated secondary antisera (Sigma), or

using the Odyssey infrared system (Licor, Lincoln, NE, USA). Briefly, cells for lysis were washed in PBS and lysed for 40 min in 3T3 extraction buffer (1% (v/v) Triton X-100, 10% (v/v) glycerol, 25 mM HEPES, 2.5 mM EDTA, 150 mM NaCl, 50 mM NaF and 30 mM NaPPi) treated with protease inhibitor cocktail (Roche). Insoluble material was removed by centrifuge at 14 000 g, and pre-cleared with protein G-conjugated sepharose beads for 30 min at 4 °C. Cleared lysates were incubated with selected antisera overnight at 4 °C. Complexes were precipitated with Protein G Sepharose for 2 h at 4 °C and spun down at 3000 g. Complexes were washed three times with IP wash buffer (100 mM NaCl, 20 mM HEPES, MgCl₂ 10 mM, EDTA 2 mM and Triton X-100 0.1% (v/v)) before suspension in sample buffer and western blot analysis. For subcellular fractionation, VCaP cells were lysed in KHEM buffer (50 mM KCl, 10 mM EGTA, 2 mM MgCl₂, 1 mM dithiothreitol and 50 mM HEPES; final pH, 7.2) by disruption with a 25-G syringe. Lysates were centrifuged at 3000 g for 5 min and the resulting supernatant centrifuged at 100 000 g for 30 min to pellet the membrane-enriched fraction from the cytosolic supernatant.

Phosphodiesterase activity assay. Phosphodiesterase activity assay was performed as previously described, using 1 μM cAMP substrate and following linear rates (Marchmont and Houslay, 1980).

Immuno-fluorescence staining. Cells were fixed for 5 min in TBS (20 mM Tris-Cl pH 7.6, 150 mM NaCl, 4% paraformaldehyde, 5% sucrose), permeabilised by incubation with 0.1% Triton X-100 in TBS and blocked (10% appropriate serum and 2% BSA, 2% marvel milk in TBS). Primary antibodies were diluted to the required concentration in blocking buffer diluted 1:1 with TBS. 1:400 diluted Alexa Fluor-conjugated IgG were used for secondary visualisation.

Confocal microscopy. Confocal microscopy was carried out on live cells expressing GFP or GFP fusion proteins, or fixed samples using a Zeiss Pascal laser-scanning confocal microscope and an Axiovert 100 microscope with an × 63/1.4 NA plan apochromat lens (Zeiss, Thornwood, NY, USA) was used for imaging. Live cells were maintained in imaging glucose supplemented PBS while images were recorded.

cAMP responsive FRET. cAMP FRET probes used in this study were first characterised by Terrin *et al* (2006). cAMP responsive FRET experiments were conducted on an Olympus IX71 inverted microscope equipped with a FLUAR × 100 NA1.3 oil-immersion objective (Zeiss). The microscope was equipped with a CCD camera (Sensicam QI, PCO, Kelheim, Germany), a software-controlled monochromator (Polychrome IV, TILL Photonics, Uckfield, UK) and a beam-splitter optical device (Multispec Microimager, Optical Insights, Santa Fe, NM, USA). Images and FRET traces were acquired using MetaFluor software (Molecular Devices, Sunnyvale, CA, USA). The resulting data are expressed as % max FRET response. Background-subtracted FRET responses were measured as a ratio of 480/545-nm fluorescence emission intensities on excitation at 430 nm and expressed as a % of the maximal FRET response, where initial forskolin-stimulated responses ($\Delta R_1/R_0$, where R_1 = FRET ratio at time t (s), R_0 = FRET ratio at time zero) are represented as a % of maximum ($\Delta R_m/R_0$, where R_m = max FRET ratio, R_0 = FRET ratio at time zero). Graphs are presented as means ± standard deviation of a minimum of 15 individual cell experiments. Coverslips were held within screw-closed metal baths allowing transmission of excitation and emission light through the coverslip, whereas images were recorded. Live cells were adherent to collagen-coated coverslips were maintained in imaging saline (125 mM NaCl, 5 mM KCl, 1 mM Na₃PO₄, 1 mM MgSO₄, 20 mM HEPES, 1 mM CaCl₂, 5.5 mM Glucose 20 mM) for the duration of experimentation. FRET responses were recorded post treatment with 10 μM forskolin or forskolin supplemented with rolipram,

whereas maximum FRET response was recorded at saturated levels post 100 μM Forskolin/IBMX treatment.

Xcelligence (Roche) proliferation assay. Cell proliferation is measured as a function of changing electrical impedance as per the manufacturer's instruction and analysed using RTCA software (Roche). Values are represented by cell index numbers, which are a dimensionless unit of measurement representing the measurement of zero impedance when cells are absent and increasing as cells divide and adhere to 96-well electrode plates. Cells were plated at a density of 30 000 per well before measurement.

Dual luciferase assays. Dual-Glo Reagents were purchased from Promega and used per the manufacturer's instruction. Assays were measured using a Mithras plate reader from Berthold and expressed as a ratio of Firefly/Renilla luciferase RLU signal.

Statistics. Where data followed a Gaussian distribution the Student's two-tailed *t*-test was used, and a *P*-value of less than 0.05 was considered to be statistically significant. Where the distribution of data was observed to be skewed (as observed in box-whisker plots), the Mann-Whitney statistical test was also used. A *P*-value of less than 0.05 was considered to be statistically significant.

RESULTS

PDE4 expression in prostate cancer cell lines and xenografts. PDE4 isoforms exhibit tissue- and cell type-specific expression patterns (Houslay, 2010). To ascertain which families of PDE4 isoforms may be deregulated during prostate cancer progression 19 human prostate cancer cell lines and xenografts were selected and screened for their PDE4 content using RT-qPCR. The sample set was composed of established cell lines and xenografts including the PC346 cell line panel (Supplementary Table 2; Marques *et al*, 2006). PDE4A, PDE4B and PDE4D transcripts were detected; with PDE4D forms observed as the most highly expressed PDE4 family. By separating the prostate cancer models into AS and AI categories (10 and 9 samples, respectively), we found that PDE4D transcripts are expressed at significantly downregulated levels in the AI category (Figure 1A–C). PDE4D isoform expression was then characterised by RT-qPCR and subjected to identical AS vs AI stratification (individual sample profiles can be found in Supplementary Table 3). Our analyses show that the PDE4D3, PDE4D4 and PDE4D7 isoforms all exhibit downregulation of mRNA expression between the AS and AI groups ($P=0.02$, $P=0.02$ and $P=0.01$, respectively). PDE4D7 is the most highly expressed isoform in AS samples and undergoes the most profound reduction in transcript abundance (Figure 1D). We observed no correlation when separating the data into cell line and xenograft groupings, nor any correlation with PDE4 expression and primary vs metastatic origin.

Validation of PDE4D7 mRNA regulation at protein level. We selected the PDE4D7 isoform for further investigation due to the dramatic reduction in transcript abundance observed in AI samples. The PDE4D7 amino-acid sequence categorises it as a long PDE4D isoform, as it contains both of the UCR1 and UCR2 regulatory domains and a unique N-terminal sequence (Houslay, 2010). The general decrease in PDE4D mRNA expression is also observed at protein level by western blotting of prostate cancer cell lines using PDE4 sub-family- and isoform-specific antisera (Figure 2A). Immunoprecipitation of PDE4D7 protein from AS VCaP and AI PC3 cells also mirrored the decrease in PDE4D7 isoform mRNA abundance between AS and AI phenotypes (Figure 2B). In order to ensure the observed downregulation of PDE4 expression was physiologically relevant, PDE assays were conducted on whole-cell lysates from both VCaP and PC3 cells.

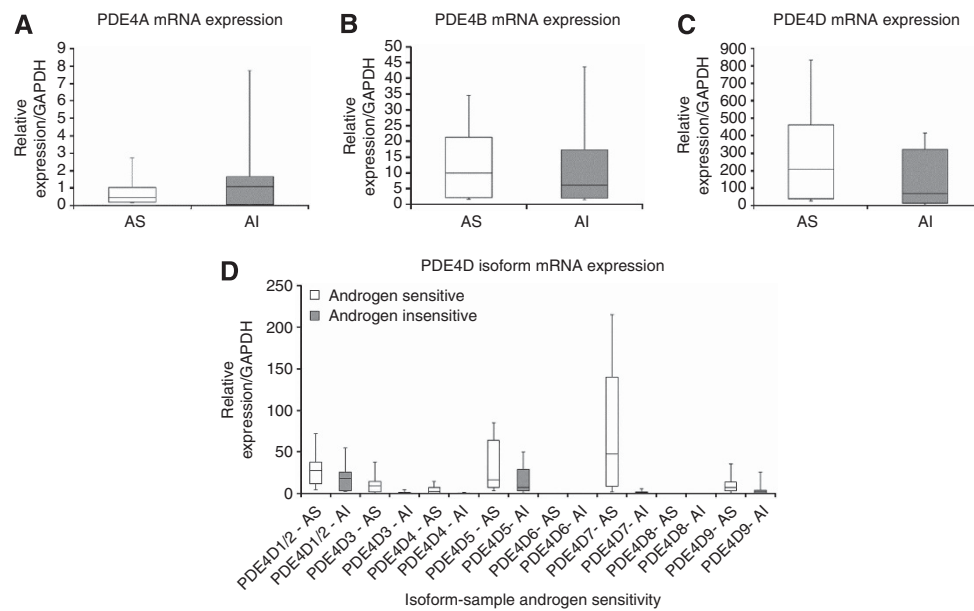


Figure 1. Box plots represent the distribution of PDE4 transcripts across 10 AS and 9 AI cell lines and xenografts. (A–C) PDE4A/B/D expression in prostate cancer cell lines and xenografts was detected by RT-qPCR. (D) PDE4D1–9 expression was assessed by RT-qPCR. PDE4D7 exhibits the highest expression of PDE4D transcripts in prostate cancer cells and is significantly downregulated in AI cells ($P=0.01$).

This enabled us to assess the impact of PDE4 downregulation on the cellular ability to degrade cAMP (Figure 2C). In doing this, we used the PDE4-selective inhibitor rolipram ($10\ \mu\text{M}$) to determine the contribution that PDE4 enzymes made to overall cAMP hydrolysis. We show that the VCaP cell line exhibits a markedly higher level of rolipram-sensitive PDE4 activity ($12.7\ \text{pmol per cAMP per min per } 1\ 000\ 000\ \text{cells}$) compared with that exhibited by PC3 cells ($0.2\ \text{pmol per cAMP per min per } 1\ 000\ 000\ \text{cells}$; $P<0.0001$). We conclude that the observed reduction in PDE4D transcript levels is recapitulated in the abundance of functional protein and may indicate a shift in cAMP signalling occurring in androgen independence.

A population of PDE4D7 localises to the sub-plasma membrane compartment of AS VCaP cells. In keeping with the PDE4D domain structure, PDE4D7 exhibits a unique N-terminal region (Wang *et al*, 2003). Given that the ‘core’ PDE4D protein is a soluble species that is found in the cytosol of cells (Bolger *et al*, 1997; Jin *et al*, 1998), these N-terminal regions define unique intracellular targeting. We therefore set out to investigate the intracellular localisation of PDE4D7 in VCaP cells. Unfortunately, the only available antisera against PDE4D7 was unsuitable for immunofluorescence. We therefore utilised PDE4D7-GFP (Figure 2D) and PDE4D7 vsv tag (Figure 2E) fusion constructs to investigate PDE4D7 sub-cellular localisation. As well as the presence of cytosolic distributed PDE4D7, we observed that a distinct population of PDE4D7 localises to the plasma membrane. In support of this observation, we also found that PDE4D7 is concentrated in the membrane-enriched fractions of VCaP cells when whole-cell lysates were separated into cytosolic and membrane-enriched preparations (Supplementary Figure 1).

PDE4D7 modulates cAMP hydrolysis at the sub-plasma membrane compartment of VCaP cells. As a fraction of PDE4D7 is targeted to the sub-plasma membrane, we wished to evaluate whether it had a role in regulating cAMP concentration at this locale as a functional signalling compartment. In order to do this, we utilised a genetically encoded FRET cAMP sensor system. A non-targeted probe that localises to the cytosol (H30) and a sensor

engineered to localise to the sub-plasma membrane (mH30) were used to comparatively investigate this sub-cellular compartmentalisation of cAMP, as described by Terrin *et al* (2006).

The adenylyl cyclase activator forskolin ($10\ \mu\text{M}$) or forskolin together with the PDE4-selective inhibitor rolipram ($10\ \mu\text{M}$) were used to assess compartmentalised PDE4 activity in FRET sensor-expressing prostate cancer cells. Maximal (100%) FRET responses were measured using a cocktail of forskolin and IBMX (each at $100\ \mu\text{M}$) to which steady-state cAMP levels for each primary treatment was compared. We uncovered that PDE4 activity has a substantial and similar role in regulating cAMP levels within both the cytosol (H30) and sub-plasma membrane compartments (mH30) of AS VCaP cells (Figure 3A and B). This is in profound contrast to AI PC3 cells, which display significantly greater FRET responses because of reduced PDE activity at the sub-plasma membrane compartment and bulk cytosol. This is in line with the significant differences in PDE activity measured by cAMP PDE assay of whole-cell lysates.

RNAi knockdown approaches have previously been used to evaluate the functional role of PDE4 sub-families and isoforms (Rampersad *et al*, 2010; Lynch *et al*, 2005). However, they inform on the total isoform population rather than just the targeted species and reduce the global rate of cAMP hydrolysis. In AS VCaP cells, we wished to determine whether plasma membrane-bound endogenous PDE4D7 contributes to the profound role we have uncovered in regulating sub-plasma membrane cAMP levels. We have previously described the use of a dominant-negative approach in several systems, where a catalytically inactive isoform is ectopically overexpressed in cells (McCahill *et al*, 2005; Ong *et al*, 2009). This acts to displace the cognate endogenous isoform from anchors that sequester it while having no effect on soluble species and the overall ability of the cell to degrade cAMP (McCahill *et al*, 2005). Using this approach, we generated a catalytically inactive form of PDE4D7 through point mutation of a single aspartic acid residue (D559A, PDE4D7). This residue lies within the catalytic site of PDE4 enzymes and has a key role in catalysis (Houslay and Adams, 2003; Huai *et al*, 2003). As a control, we also employed a catalytically inactive PDE4D3 construct (D484A, PDE4D3), as described previously (McCahill *et al*, 2005).

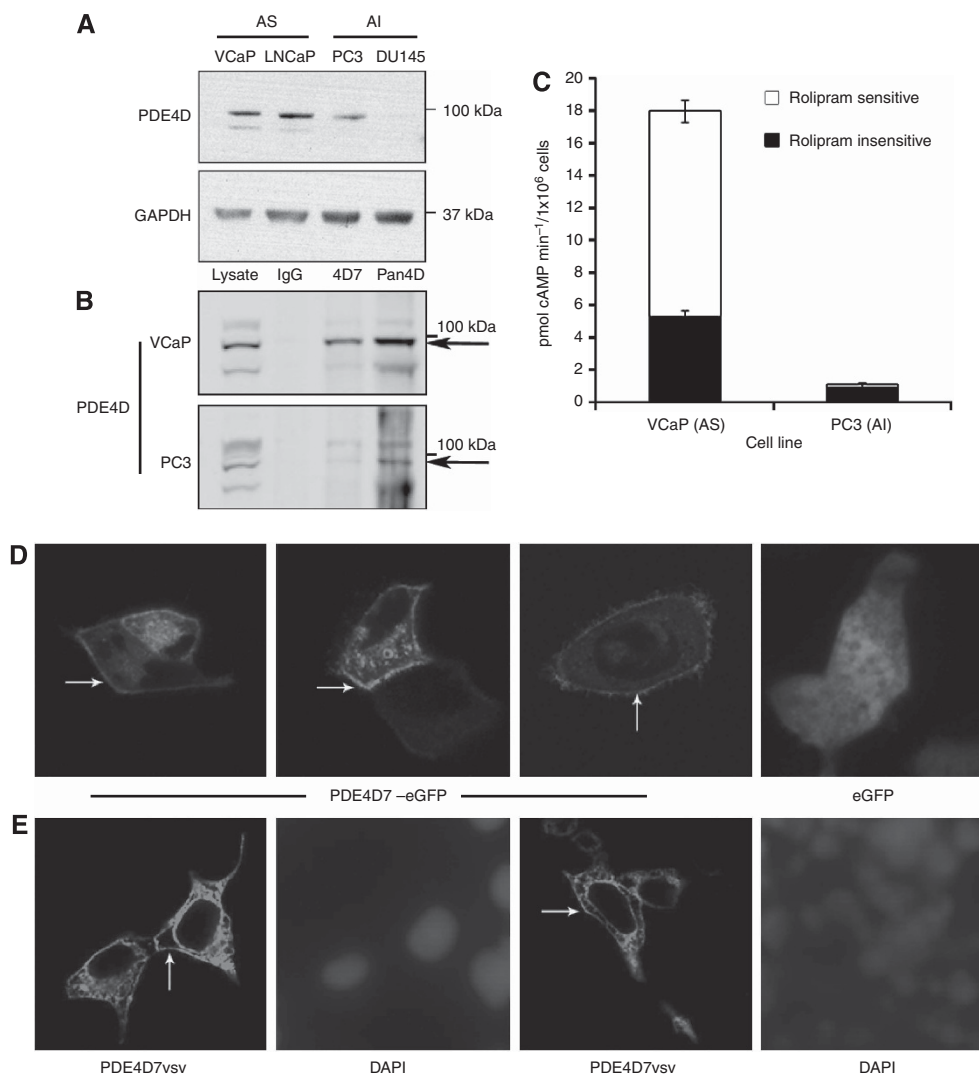


Figure 2. (A) PDE4D protein expression is reduced in the AI PC3 and DU145 cell lines compared with AS VCaP and LNCaP cells. PDE4D5 and 7 co-migrate because of similar molecular weights (upper band); PDE4D3/8/9 isoforms are represented within the lower isoform band. GAPDH expression is shown as a protein-loading control. (B) PDE4D7 and PDE4D were immunoprecipitated from VCaP and PC3 cells. PDE4D7 molecular weight is highlighted by the positioning of a black arrow. PDE4D7 protein expression is higher in VCaP cells than in PC3. (C) Overall PDE activity is significantly higher in the VCaP cell line in comparison to PC3 cells ($P < 0.0001$). Rolipram-sensitive PDE4 hydrolysis (white bar) and non-PDE4 cAMP hydrolysis (black bar) are represented as pmol cAMP per min per 1 000 000 cells. (D and E) GFP- and VSV-tagged PDE4D7 expressed in VCaP cells. A population of each fusion protein was observed at the sub-plasma membrane compartment. Where eGFP-PDE4D7 was imaged in living cells monomeric eGFP was used as a comparison. White arrows indicate populations of PDE4D7vsv at the plasma membrane.

VCaP cells co-expressing catalytically inactive PDE4D and cAMP-responsive FRET constructs were then used to investigate if forskolin-induced localised cAMP accumulation is exacerbated by dislodging endogenous PDE4D7 from native anchoring sites (Figure 3C). We found that displacing PDE4D7 severely disrupted localised cAMP hydrolysis at the plasma membrane as shown by a significant increase in the mH30 FRET response. In contrast, similar levels of ectopically expressed inactive PDE4D3 had no effect on the ability of forskolin to cause cAMP accumulation at the plasma membrane compartment (Figure 3C–F). This dominant-negative induced response was only observed using the plasma membrane associated probe and was not detected in the cytosol. These data indicate that catalytically inactive PDE4D7 specifically displaces members of an endogenous, active PDE4D7 population from the plasma membrane and that PDE4D7 has a major role in regulating sub-plasma membrane cAMP levels in prostate cancer cells.

PDE4D7 regulates prostate cancer proliferation. The impact of PDE4D7-mediated cAMP hydrolysis on cellular proliferation was then examined in order to assess if the downregulation of PDE4D7 expression during the onset of the AI phenotype impacted on proliferation rate. Dominant-negative PDE4D7 expression was employed in order to observe how the displacement of PDE4D7 from endogenous anchoring sites and the accumulation of cAMP at the plasma membrane-affected VCaP proliferation. The catalytically active wild-type PDE4D7 was used in comparison to dominant-negative expression (Figure 4C). We found that expression of the inactive PDE4D7 led to a marked increase in VCaP cell proliferation rate ($P = 0.02$).

Having found that displacement of PDE4D7 was sufficient to elicit an increase in proliferation, we then decided to investigate if downregulation of PDE4D7 would have similar results. We utilised specific siRNA-mediated knockdown of global PDE4D7 and found that depletion of the isoform led to an increase in proliferation rate

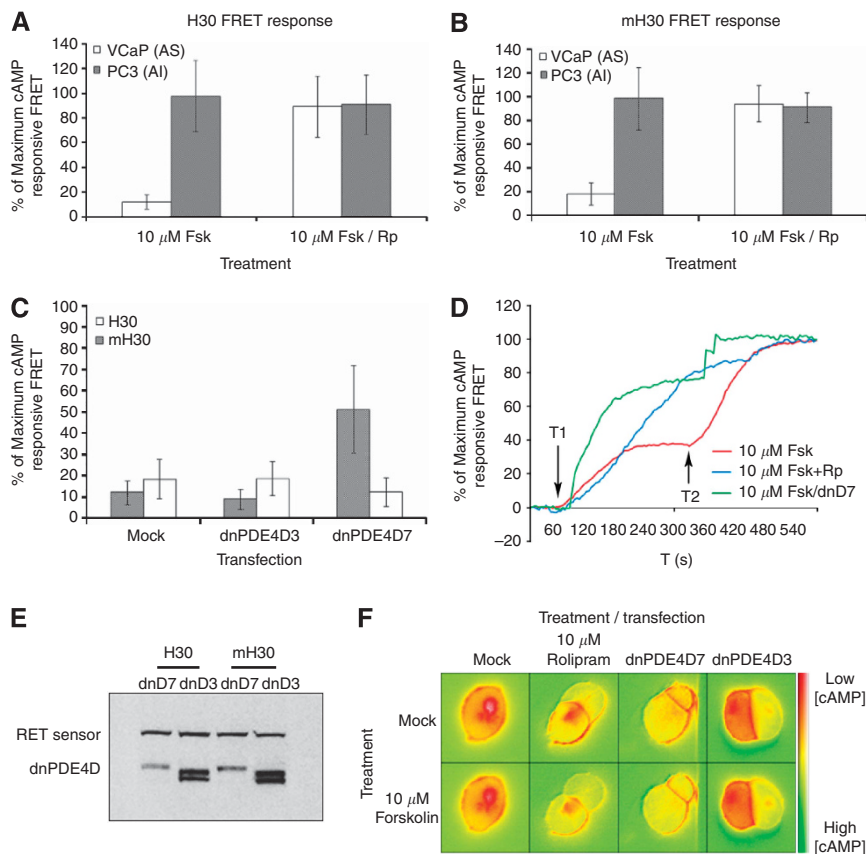


Figure 3. (A and B) cAMP responsive FRET analysis shows that rolipram-sensitive PDE4 activity suppresses cAMP accumulation induced by 10 μM forskolin in VCaP cells (white bars, $P < 0.01$). This PDE4-mediated cAMP degradation is observed in the cytosol (A—H30) and at the plasma membrane (B—mH30) of the AS cell line. PC3 cells (shaded bars) exhibited negligible attenuation of cAMP concentration at the bulk cytosol or at the plasma membrane in response to 10 μM forskolin (Fsk) or forskolin/rolipram (Fsk/Rp) treatment. (C) PDE4D7 constrains cAMP accumulation at the plasma membrane of VCaP cells. Dominant-negative PDE4D (dnPDE4D7) isoform expression has no significant impact on the ability of VCaP cells to control global cAMP accumulation in the bulk cytosol in response to 10 μM forskolin treatment (white bars). The mH30 construct (shaded bars) exhibited a significant change in FRET response (~30% over mock transfection) when the reporter construct was co-transfected with dominant-negative PDE4D7 ($P < 0.01$). Dominant-negative PDE4D3 (dnPDE4D3) expression elicited no significant change in FRET response over mock transfection. (D) Example FRET traces depicting the significant effect of dnPDE4D7 on the plasma membrane cAMP dynamics in comparison to forskolin (Fsk) and forskolin/rolipram (Fsk/Rp) treatment of VCaP cells. T1 and T2 denote treatment times for the forskolin alone trace where the addition of 10 μM forskolin is shown by T1 and T2 indicates the addition of 100 μM forskolin/IBMX. (E) H30 FRET sensors and PDE4D constructs were expressed in at equivalent levels in VCaP cells as assessed by western blot analysis. Upper bands represent the FRET probes, whereas lower bands represent transfected PDE4D constructs. (F) Example pseudo-colour images depicting the change in FRET response upon 10 μM forskolin treatment and dominant-negative expression in VCaP cells expressing mH30.

over and above that observed for global PDE4D depletion ($P = 0.06$). This further indicates a specialised role for the PDE4D7 isoform in prostate cell biology (Figure 4F). The efficiency of siRNA-mediated protein knockdown was assessed for each oligonucleotide using western blot densitometry (Supplementary Figure 2).

We next investigated whether re-expression of PDE4D7 in PC3 cells was sufficient to impede cell proliferation. Overexpression of wild-type PDE4D7 resulted in a significant decrease in PC3 cell proliferation ($P < 0.01$), indicating that PDE4D7-mediated cAMP degradation within the AI cells results in inhibition of proliferative signalling events (Figure 3G–I). To substantiate if increased cAMP signalling facilitates a growth advantage in the AI phenotype, we then stimulated PC3 cells with the adenylyl cyclase activator, forskolin (10 μM) and observed a marked increase in proliferation rate, which was insensitive to treatment with the PDE4 inhibitor rolipram (10 μM; Supplementary Figure 3). The lack of response to rolipram is consistent with our findings that PDE4 activity and

PDE4D7 expression is downregulated in PC3 cells, and further suggests a growth advantage is imparted by suppression of PDE4D7 expression and increased cAMP signalling.

PDE4D7 is not directly regulated by the androgen receptor.

Bioinformatic EST sequence inspection reveals that the PDE4D7 transcript encodes a UTR that maps to a genomic region overlapping antisense with a previously characterised androgen-regulated gene, namely *PART1* (Lin *et al*, 2000; Sidiropoulos *et al*, 2001; ESTs DA627904, DB213544, DB22103, DB224202, DB226810, DB230503, DB237063 and DR003683; Figure 5A). We also found that *PART1* and *PDE4D7* mRNA share similar levels of expression within a sample set of prostate cancer cell lines and xenografts (Figure 5B). Given the decrease in *PDE4D7* mRNA abundance in AI samples and the genomic relationship to *PART1*, we felt it important to assess whether *PDE4D7* expression is regulated by the androgen receptor. Using luciferase reporter constructs, we found that the promoter region of *PDE4D7*

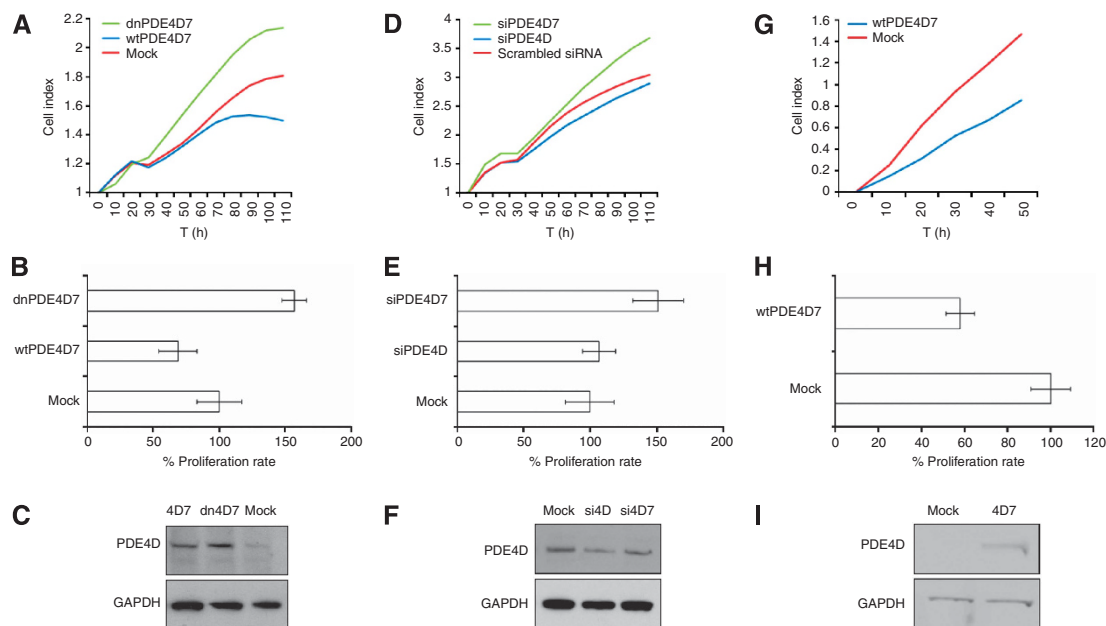


Figure 4. (A and B) PDE4D7 regulates prostate cancer cellular proliferation in VCaP cells. Proliferation was measured using the electrical impedance-based Xcelligence system from Roche. The exogenous expression of the dominant-negative PDE4D7 in VCaP cells induces a 50% increase in proliferation rate over wtPDE4D7 and mock control experiments ($P=0.02$). **(C)** Dominant-negative and wild-type PDE4D7 constructs were expressed at equivalent levels in VCaP cells as assessed by western blot analysis using antisera against PDE4D. GAPDH was used as a control for equivalent protein loading. **(D and E)** The proliferation of VCaP cells was measured in response to siRNA-mediated knockdown of PDE4D7. PDE4D7 knockdown increases VCaP proliferation rate over mock and pan PDE4D siRNA ($P=0.06$). **(F)** siRNA knockdown of PDE4D and PDE4D7 decreased the abundance of endogenous expression as assessed by western blot analysis. **(G and H)** Transfection of wtPDE4D7 into PC3 cells significantly decreased cellular proliferation over mock transfection ($P<0.01$). **(I)** PDE4D7 expression in PC3 cells was assessed by western blot analysis, using GAPDH expression as a control for equivalent protein loading.

(PDE4D7 γ) exhibited no response to androgen stimulation in VCaP cells, but was activated by increased intracellular calcium levels induced by ionomycin ($3\mu\text{M}$), presumably due to the presence of a putative NFAT-binding motif within the PDE4D7 promoter (5'-GGAAAATcctgtATTTTCC-3', 500 bp upstream of NM_001165899.1 exon 1; Figure 5C).

To assess if long-range androgen receptor enhancer elements impacted PDE4D7 expression, a series of steroid deprivation and androgen response experiments were performed on the VCaP cell line. Prostate-specific antigen (PSA) and PART-1 transcript levels were used as a measure of androgen receptor activity, whereas chromogranin A and neurone-specific enolase mRNA were measured to assess the neuroendocrine differentiation commonly associated with steroid ablation of AS cell lines (Amorino and Parsons, 2004). PDE4D5 transcript levels were measured alongside PDE4D7 in order to investigate if any observed change in transcript abundance was specific to PDE4D7, or common to other PDE4D long isoforms expressed in prostatic cells. As expected, 48 h of exposure to media supplemented with charcoal-stripped serum led to a decrease in the expression of the androgen-regulated PSA and PART-1 transcripts, whereas neurone-specific enolase and chromogranin A expression increased (Figure 5D). PSA and PART-1 transcript levels were upregulated by treatment with the androgen receptor agonist, dihydrotestosterone (10 nM , 48 h treatment) and inhibition of the androgen receptor by the antagonist, hydroxyflutamide ($1\mu\text{M}$, 48 h treatment) led to a decrease in PSA transcription activity. These data indicate that transcription from the *PDE4D7* locus is not directly regulated by the androgen receptor, unlike the *PDE4D7* cis-natural antisense transcript, *PART1*. It is therefore an intriguing possibility that PDE4D7 expression may be epigenetically modulated, as PDE4D

promoters have been shown to be alternately methylated in a tissue-dependent and temporally regulated manner during mouse embryo development (Huang *et al*, 2013).

DISCUSSION

The role of tightly regulated cAMP signalling cascades in cellular function and tissue homeostasis is underpinned by the enzymatic activity of cAMP PDEs (Houslay *et al*, 2007, 2010). As PDEs have a pivotal role in determining intracellular cAMP concentrations and where tethered populations shape gradients of cAMP thereby underpinning compartmentalisation, then we can expect that inappropriate changes in PDE expression and activity will lead to alterations in the balance of signalling events mediated by cyclic nucleotides that may then facilitate disease state progression. cAMP-mediated signalling pathways within the prostate have long been connected with epithelial tumorigenesis and cancer progression (Cho-Chung and Nesterova, 2005; Merkle and Hoffmann, 2011; Zhang *et al*, 2011; Sarwar *et al*, 2013). Synergy between the AR and protein kinase A in AS cells can lead to an increase in the transcription of androgen-regulated genes and under some circumstances lead to transactivation of the AR and cellular differentiation (Komiya *et al*, 2009; Desiniotis *et al*, 2010). There is also evidence to suggest that the more advanced phenotypes of AI prostate cancer also become more dependent upon cAMP signalling as cells shift from steroidal to non-steroidal growth factor signalling pathways in response to androgen deprivation treatments (Gutierrez-Canas *et al*, 2003; Desiniotis *et al*, 2010; Flacke *et al*, 2013). In this light, it is interesting that we find PDE4

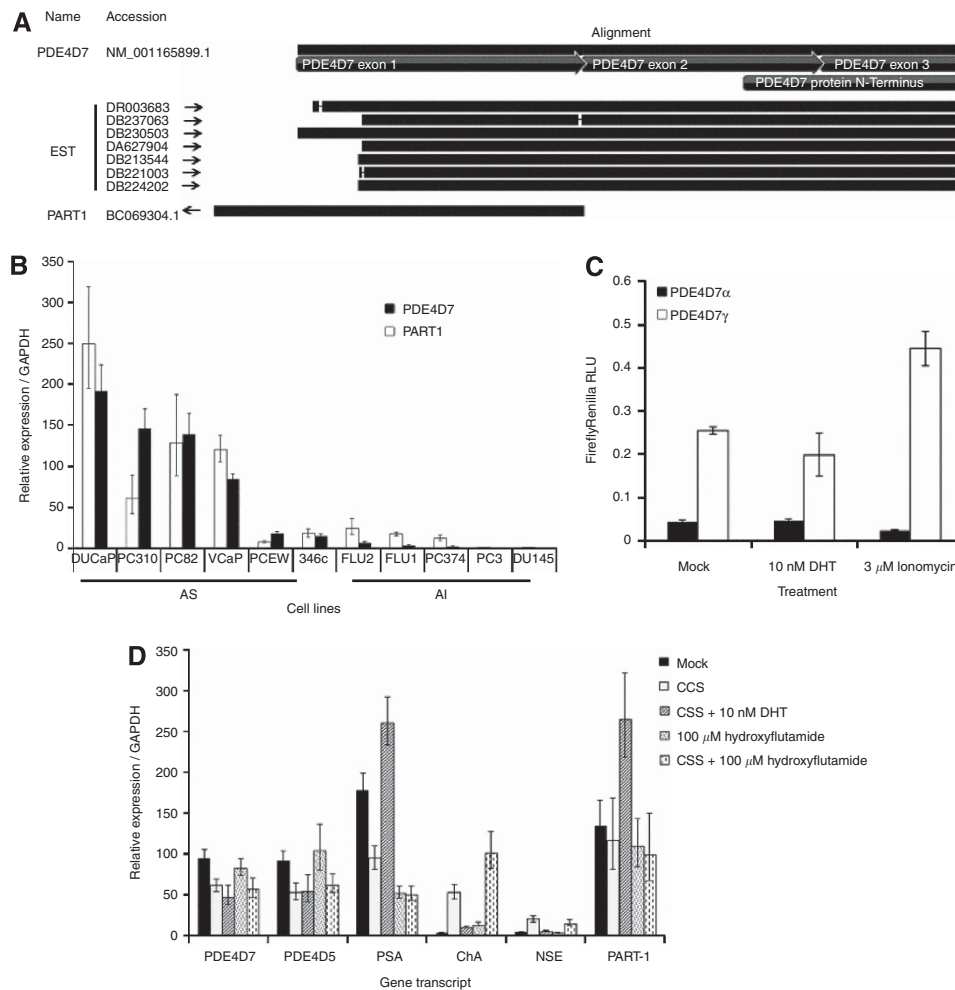


Figure 5. (A) Sequence alignment of PDE4D7 and PART1 mRNA against a selection of EST sequences. The 5' UTR of the PDE4D7 transcript is encoded by two exons the first of which overlaps with a distal androgen-responsive gene, PART1. The exon numbering of PDE4D7 refers to that of the 3 exons involved in encoding the unique N-terminal region of PDE4D7 mRNA and not to any of the 14 common exons involved in forming all of the various PDE4D isoforms, which are usually denoted as exon-2 through to exon-15. **(B)** PDE4D7 and PART1 mRNA expression share a positive correlation prostate cancer cell lines and xenografts ($R=0.79$). **(C)** The proximal 2 kb of the PDE4D7 promoter region (PDE4D7/PART1 locus—PDE4D7 γ) is not stimulated by 12 h of 10 nM DHT treatment of VCaP cells, but exhibits a mild response to increased intracellular calcium levels induced by 12 h of 3 μM ionomycin treatment. Results are compared against a 1-kb fragment of DNA cloned from upstream of PDE4D7 exon 2 (PDE4D locus—PDE4D7 α) and are displayed as relative light units normalised to the activity Renilla luciferase driven by a constitutively active viral thymidine kinase promoter reference construct. **(D)** PDE4D7 transcript levels were not affected by modulation of the androgen receptor in VCaP cells. PSA and PART1 transcripts display the expected increase in expression in response to 10 nM DHT exposure and decrease in repose to hormone deprivation or AR inhibition, whereas PDE isoforms showed no significant change in expression.

isoforms are highly expressed in AS prostate cancer cells and significantly downregulated in AI cells, and that we can attribute a significant proportion of this decrease to a single PDE4 isoform, namely PDE4D7.

Previous work by Ückert *et al* (2001, 2006) explored the expression of PDE families in the histological zones of the prostate by using RT-PCR, immunofluorescence and selective PDE inhibitors. They found that multiple PDE families, including PDE4, are present within the different histological zones of the prostate and noting significant PDE4 expression within the luminal epithelia. However, the complexity of isoform expression and cell-specific transcription were not addressed during their investigation. A more recent study further connected the increased expression of the PDE4D sub-family with prostatic tumorigenesis (Rahrman *et al*, 2009). A *T2/onc* transposon insertion at the *PDE4D* gene (resulting in the putative overexpression of short-form PDE4Ds but potentially disrupting PDE4D long forms) potentiated the neoplasia of prostatic epithelial cells. This is particularly interesting

with regards to the observed high expression of PDE4 mRNA in AS samples (an observation also made in patient materials by Rahrman *et al*) and is in line with a recent study indicating that *PDE4D* homozygous deletion or micro-deletions within the gene paradoxically lead to an increase in expression and promote cancer of many types (Lin *et al*, 2013). However, this does not explain the downregulation of PDE4 mRNA in the AI phenotype nor address the importance of isoform specificity to tumorigenesis and cancer progression.

The tethering of PDE isoforms to specific sub-cellular locales via isoform-specific N-terminal and conserved regulatory domains allows for the paradigm of compartmentalised cAMP dynamics to explain how multiple independent cAMP signalling events can occur simultaneously (Houslay, 2010). PDE4D7 follows in this paradigm by being tethered to and constraining cAMP accumulation at the plasma membrane. This is the first functional activity attributed to this long PDE4D7 isoform, although it is akin to other long-form PDE4D isoforms such as PDE4D3 and PDE4D5, which

have been demonstrated to control distinct cellular processes through selective association with signalling scaffolds (Lynch *et al*, 2005; Terrin *et al*, 2012). The positioning of PDE4D7 tethers it in prime position to regulate the activities of plasma membrane-bound adenylyl cyclases and therefore mediate G_s-coupled GPCR signal transduction across the plasma membrane. The increased proliferation rate of VCaP cells when PDE4D7 is displaced or disrupted does indicate that the isoform mediates proliferative signalling, which with downregulation of endogenous PDE4D7 could increasingly become over-active and ultimately contribute to the AI phenotype by exacerbating the paracrine and autocrine signalling loops, which can sustain AR transactivation and AI growth of prostate cancer cells (Gutierrez-Canas *et al*, 2003). Interestingly, up until this evaluation, little or nothing was known about the properties of PDE4D7 despite the fact that susceptibility markers for ischemic stroke map to the region of Chr5q12 where PDE4D7 and the overlapping PART1 exons locate (Gretarsdottir *et al*, 2003). The cardiogenic/carotid stroke-associated haplotype was shown to extend over the region encoding the N-terminal region unique to PDE4D7 as well as its putative promoter regions, which led to a lowered PDE4D7 expression in stroke. Importantly, it has been shown that overall mortality was 20% higher in prostate cancer patients with pre-existing stroke compared with those without and that different forms of androgen-deprivation therapy may increase the risk of stroke/transient ischaemic attacks (Jespersen *et al*, 2011; Razzak, 2012).

PDE4D7 has potential as a promising target for use as a biomarker in prostate cancer. Its high expression in AS cells, coupled with its subsequent decline into AI cells may provide a novel modular marker that could be used to diagnose disease stage. An analysis of PDE4D7 expression from extended numbers of patient-derived prostatic cancers would be required to validate its use as a clinically effective biomarker and to elucidate any correlative potential that PDE4D7 expression may have with patient survival and likelihood of disease progression. Moreover, if high PDE4D7 expression is a contributing factor to early tumorigenesis, then pharmacological modulation of its activity may be beneficial, although this would have to be balanced against increases in cAMP signalling and induction of AI cells (Lin *et al*, 2013).

We conclude that (i) PDE4D7 is differentially regulated between AS and AI disease and this is independent of canonical AR signalling. (ii) PDE4D has a significant role in prostatic cAMP hydrolysis and cell proliferation. (iii) PDE4D7 has the potential to be used as a novel biomarker for diagnosis of the transition to AI prostate cancer, and that manipulation of PDE4D7 activity or expression could usefully be investigated further for its therapeutic potential.

ACKNOWLEDGEMENTS

We thank Professor M Zaccolo (Oxford, UK) for supplying the cAMP FRET probes used within this study. We also acknowledge the support provided by the Biotechnology and Biological Sciences Research Council (UK) for award of a CASE studentship to David JP Henderson. This study was supported by the framework of CTMM (The Netherlands), the Center for Translational Molecular Medicine, PCMM project (grant 03O-203). BBSRC funding to GSB (BB/G01647X/1).

REFERENCES

Amorino GP, Parsons SJ (2004) Neuroendocrine cells in prostate cancer. *Crit Rev Eukaryot Gene Expr* **14**(4): 287–300.

- Bolger G, Erdogan S, Jones R, Loughney K, Scotland G, Hoffmann R, Wilkinson I, Farrell C, Houslay M (1997) Characterization of five different proteins produced by alternatively spliced mRNAs from the human cAMP-specific phosphodiesterase PDE4D gene. *Biochem J* **328**(2): 539–548.
- Cho-Chung YS, Nesterova MV (2005) Tumor reversion: protein kinase A isozyme switching. *Ann N Y Acad Sci* **1058**(1): 76–86.
- Conti M, Beavo J (2007) Biochemistry and physiology of cyclic nucleotide phosphodiesterases: essential components in cyclic nucleotide signaling. *Annu Rev Biochem* **76**: 481–511.
- Desinotias A, Schäfer G, Klocker H, Eder IE (2010) Enhanced antiproliferative and proapoptotic effects on prostate cancer cells by simultaneously inhibiting androgen receptor and cAMP-dependent protein kinase A. *Int J Cancer* **126**(3): 775–789.
- Feldman BJ, Feldman D (2001) The development of androgen-independent prostate cancer. *Nat Rev Cancer* **1**(1): 34–45.
- Flacke J-P, Flacke H, Appukuttan A, Palisaar R-J, Noldus J, Robinson BD, Reusch HP, Zippin JH, Ladilov Y (2013) Type 10 soluble adenylyl cyclase is overexpressed in prostate carcinoma and controls proliferation of prostate cancer cells. *J Biol Chem* **288**(5): 3126–3135.
- Foley R, Marignol L, Keane JP, Lynch TH, Hollywood D (2011) Androgen hypersensitivity in prostate cancer: Molecular perspectives on androgen deprivation therapy strategies. *Prostate* **71**(5): 550–557.
- Francis SH, Blount MA, Corbin JD (2011) Mammalian cyclic nucleotide phosphodiesterases: molecular mechanisms and physiological functions. *Physiol Rev* **91**(2): 651–690.
- Gretarsdottir S, Thorleifsson G, Reynisdottir S, Manolescu A, Jonsdottir S, Jonsdottir T, Gudmundsdottir T, Bjarnadottir S, Einarsson O, Gudjonssdottir H, Hawkins M, Gudmundsson G, Gudmundsdottir H, Andrason H, Gudmundsdottir A, Sigurdardottir M, Chou T, Nahmias J, Goss S, Sveinbjornsdottir S, Valdimarsson E, Jakobsson F, Agnarsson U, Gudnason V, Thorgeirsson G, Fingerle J, Gurney M, Gudbjartsson D, Frigge M, Kong A, Stefansson K, Gulcher J (2003) The gene encoding phosphodiesterase 4D confers risk of ischemic stroke. *Nat Genet* **37**(5): 131–138.
- Grignon DJ, Sakr WA (1994) Zonal origin of prostatic adenocarcinoma: are there biologic differences between transition zone and peripheral zone adenocarcinomas of the prostate gland? *J Cell Biochem Suppl* **19**: 267–269.
- Gutierrez-Canas I, Rodriguez-Henche N, Bolanos O, Carmena M, Prieto J, Juarranz M (2003) VIP and PACAP are autocrine factors that protect the androgen-independent prostate cancer cell line PC-3 from apoptosis induced by serum withdrawal. *Br J Pharmacol* **139**(5): 1050–1058.
- Houslay M, Baillie G, Maurice D (2007) cAMP-specific phosphodiesterase-4 enzymes in the cardiovascular system—a molecular toolbox for generating compartmentalized cAMP signaling. *Circ Res* **100**(7): 950–966.
- Houslay MD (2010) Underpinning compartmentalised cAMP signalling through targeted cAMP breakdown. *Trends Biochem Sci* **35**(2): 91–100.
- Houslay MD, Adams DR (2003) PDE4 cAMP phosphodiesterases: modular enzymes that orchestrate signalling cross-talk, desensitization and compartmentalization. *Biochem J* **370**(1): 1–18.
- Huai Q, Colicelli J, Ke H (2003) The crystal structure of AMP-bound PDE4 suggests a mechanism for phosphodiesterase catalysis†,‡. *Biochemistry* **42**(45): 13220–13226.
- Huang Z, Han Z, Cui W, Zhang F, He H, Zeng T, Sugimoto K, Wu Q (2013) Dynamic expression pattern of Pde4d and its relationship with CpG methylation in the promoter during mouse embryo development. *Biochem Biophys Res Commun* **441**(4): 982–987.
- Huston E, Houslay T, Baillie G, Houslay M (2006) cAMP phosphodiesterase-4A1 (PDE4A1) has provided the paradigm for the intracellular targeting of phosphodiesterases, a process that underpins compartmentalized cAMP signalling. *Biochem Soc Trans* **34**: 504–509.
- Jespersen C, Norgaard M, Bjerklund Johansen T, Sogaard M, Borre M (2011) The influence of cardiovascular morbidity on the prognosis in prostate cancer. Experience from a 12-year nationwide Danish population-based cohort study. *BMC Cancer* **11**(1): 519.
- Jin S, Bushnik T, Lan L, Conti M (1998) Subcellular localization of rolipram-sensitive, cAMP-specific phosphodiesterases—differential targeting and activation of the splicing variants derived from the PDE4D gene. *J Biol Chem* **273**(31): 19672–19678.
- Kasbohm EA, Guo R, Yowell CW, Bagchi G, Kelly P, Arora P, Casey PJ, Daaka Y (2005) Androgen receptor activation by G(s) signaling in prostate cancer cells. *J Biol Chem* **280**(12): 11583–11589.

- Keravis T, Lugnier C (2010) Cyclic nucleotide phosphodiesterases (PDE) and peptide motifs. *Curr Pharm Design* **16**(9): 1114–1125.
- Komiya A, Suzuki H, Imamoto T, Kamiya N, Nihei N, Naya Y, Ichikawa T, Fuse H (2009) Neuroendocrine differentiation in the progression of prostate cancer. *Int J Urol* **16**(1): 37–44.
- Kvissel A-K, Ramberg H, Eide T, Svindland A, Skålhegg BS, Taskén KA (2007) Androgen dependent regulation of protein kinase A subunits in prostate cancer cells. *Cell Signal* **19**(2): 401–409.
- Lin B, White JT, Ferguson C, Bumgarner R, Friedman C, Trask B, Ellis W, Lange P, Hood L, Nelson PS (2000) PART-1: A novel human prostate-specific, androgen-regulated gene that maps to chromosome 5q12. *Cancer Res* **60**(4): 858–863.
- Lin DC, Xu L, Ding LW, Sharma A, Liu LZ, Yang H, Tan P, Vadgama J, Karlan BY, Lester J, Urban N, Schummer M, Doan N, Said JW, Sun HM, Walsh M, Thomas CJ, Patel P, Yin D, Chan D, Koeffler HP (2013) Genomic and functional characterizations of phosphodiesterase subtype 4D in human cancers. *Proc Natl Acad Sci USA* **110**(15): 6109–6114.
- Lynch M, Baillie G, Houslay M (2007) cAMP-specific phosphodiesterase-4D5 (PDE4D5) provides a paradigm for understanding the unique non-redundant roles that PDE4 isoforms play in shaping compartmentalized cAMP cell signalling. *Biochem Soc Trans* **35**: 938–941.
- Lynch MJ, Baillie GS, Mohamed A, Li X, Maisonneuve C, Klussmann E, van Heeke G, Houslay MD (2005) RNA silencing identifies PDE4D5 as the functionally relevant cAMP phosphodiesterase interacting with beta arrestin to control the protein kinase A/AKAP79-mediated switching of the beta2-adrenergic receptor to activation of ERK in HEK293B2 cells. *J Biol Chem* **280**(39): 33178–33189.
- MacKenzie KF, Wallace DA, Hill EV, Anthony DF, Henderson DJP, Houslay DM, Arthur JSC, Baillie GS, Houslay MD (2011) Phosphorylation of cAMP-specific PDE4A5 (phosphodiesterase-4A5) by MK2 (MAPKAPK2) attenuates its activation through protein kinase A phosphorylation. *Biochem J* **435**(3): 755–769.
- MacKenzie S, Baillie G, McPhee I, MacKenzie C, Seamons R, McSorley T, Millen J, Beard M, van Heeke G, Houslay M (2002) Long PDE4 cAMP specific phosphodiesterases are activated by protein kinase A-mediated phosphorylation of a single serine residue in Upstream Conserved Region 1 (UCR1). *Br J Pharmacol* **136**(3): 421–433.
- Marchmont RJ, Houslay MD (1980) A Peripheral and intrinsic enzyme constitute the cyclic-AMP phosphodiesterase activity of rat-liver plasma-membranes. *Biochem J* **187**(2): 381–392.
- Marques RB, van Weerden WM, Erkens-Schulze S, de Ridder CM, Bangma CH, Trapman J, Jenster G (2006) The human PC346 xenograft and cell line panel: a model system for prostate cancer progression. *Eur Urol* **49**(2): 245–257.
- McCahill A, McSorley T, Huston E, Hill EV, Lynch MJ, Gall I, Keryer G, Lygren B, Tasken K, van Heeke G, Houslay MD (2005) In resting COS1 cells a dominant negative approach shows that specific, anchored PDE4 cAMP phosphodiesterase isoforms gate the activation, by basal cyclic AMP production, of AKAP-tethered protein kinase A type II located in the centrosomal region. *Cell Signal* **17**(9): 1158–1173.
- Merkle D, Hoffmann R (2011) Roles of cAMP and cAMP-dependent protein kinase in the progression of prostate cancer: cross-talk with the androgen receptor. *Cell Signal* **23**(3): 507–515.
- Murdoch H, Vadrevu S, Prinz A, Dunlop AJ, Klussmann E, Bolger GB, Norman JC, Houslay MD (2011) Interaction between LIS1 and PDE4, and its role in cytoplasmic dynein function. *J Cell Sci* **124**(13): 2253–2266.
- Ong W, Gribble F, Reimann F, Lynch M, Houslay M, Baillie G, Furman B, Pyne N (2009) The role of the PDE4D cAMP phosphodiesterase in the regulation of glucagon-like peptide-1 release. *Br J Pharmacol* **157**(4): 633–644.
- Rahrmann EP, Collier LS, Knutson TP, Doyal ME, Kuslak SL, Green LE, Malinowski RL, Roethe L, Akagi K, Waknitz M, Huang W, Largaespada DA, Marker PC (2009) Identification of PDE4D as a Proliferation Promoting Factor in Prostate Cancer Using a Sleeping Beauty Transposon-Based Somatic Mutagenesis Screen. *Cancer Res* **69**(10): 4388–4397.
- Rampersad S, Owens J, Huston E, Umama M, Wilson L, Netherton S, Lynch M, Baillie G, Houslay M, Maurice D (2010) Cyclic AMP phosphodiesterase 4D (PDE4D) tethers EPAC1 in a vascular endothelial cadherin (VE-Cad)-based signaling complex and controls cAMP-mediated vascular permeability. *J Biol Chem* **285**(44): 33614–33622.
- Razzak M (2012) Prostate cancer: cardiovascular risk and androgen deprivation therapy. *Nat Rev Urol* **9**(2): 61–61.
- Sarwar M, Sandberg S, Abrahamsson P-A, Persson JL (2013) Protein kinase A (PKA) pathway is functionally linked to androgen receptor (AR) in the progression of prostate cancer. *Urol Oncol* **12**(0): 1078–1439.
- Sidiropoulos M, Chang A, Jung K, Diamandis EP (2001) Expression and regulation of prostate androgen regulated transcript-1 (PART-1) and identification of differential expression in prostatic cancer. *Br J Cancer* **85**(3): 393–397.
- Siegel R, Naishadham D, Jemal A (2013) Cancer statistics, 2013. *CA Cancer J Clin* **63**(1): 11–30.
- Terrin A, Di Benedetto G, Pertegato V, Cheung YF, Baillie G, Lynch MJ, Elvassore N, Prinz A, Herberg FW, Houslay MD, Zaccolo M (2006) PGE(1) stimulation of HEK293 cells generates multiple contiguous domains with different cAMP: role of compartmentalized phosphodiesterases. *J Cell Biol* **175**(3): 441–451.
- Terrin A, Monterisi S, Stangherlin A, Zoccarato A, Koschinski A, Surdo NC, Mongillo M, Sawa A, Jordanides NE, Mountford JC, Zaccolo M (2012) PKA and PDE4D3 anchoring to AKAP9 provides distinct regulation of cAMP signals at the centrosome. *J Cell Biol* **198**(4): 607–621.
- Wang D, Deng C, Bugaj-Gaweda B, Kwan M, Gunwaldsen C, Leonard C, Xin X, Hu Y, Unterbeck A, De Vivo M (2003) Cloning and characterization of novel PDE4D isoforms PDE4D6 and PDE4D7. *Cell Signal* **15**(9): 883–891.
- Wang X, Julio MK-d, Economides KD, Walker D, Yu H, Halili MV, Hu Y-P, Price SM, Abate-Shen C, Shen MM (2009) A luminal epithelial stem cell that is a cell of origin for prostate cancer. *Nature* **461**(7263): 495–500.
- Wegiel B, Evans S, Hellsten R, Otterbein LE, Bjartell A, Persson JL (2010) Molecular pathways in the progression of hormone-independent and metastatic prostate cancer. *Curr Cancer Drug Targets* **10**(4): 392–401.
- Zhang P, He X, Tan J, Zhou X, Zou L (2011) β -Arrestin2 mediates β -2 adrenergic receptor signaling inducing prostate cancer cell progression. *Oncol Rep* **26**(6): 1471–1477.
- Ückert S, Kütke A, Jonas UDO, Stief CG (2001) Characterisation and functional relevance of cyclic nucleotide phosphodiesterase isoenzymes of the human prostate. *J Urol* **166**(6): 2484–2490.
- Ückert S, Oelke M, Stief CG, Andersson KE, Jonas U, Hedlund P (2006) Immunohistochemical distribution of cAMP- and cGMP-phosphodiesterase (PDE) isoenzymes in the human prostate. *Eur Urol* **49**(4): 740–745.

This work is published under the standard license to publish agreement. After 12 months the work will become freely available and the license terms will switch to a Creative Commons Attribution-NonCommercial-Share Alike 3.0 Unported License.

Supplementary Information accompanies this paper on British Journal of Cancer website (<http://www.nature.com/bjc>)